A Resolution-Enhanced Sliding Matrix Pencil Method for Evaluation of Harmonics Distortion in Shipboard Microgrids

Yacine Terriche, Muhammad Umair Mutarraf, *Student Member, IEEE*, Abderrzak Laib, Chun-Lien Su, *Senior Member, IEEE*, Josep M. Guerrero, *Fellow, IEEE*, Juan C. Vasquez, *Senior Member, IEEE*, and Saeed Golestan, *Senior Member, IEEE*

***Abstract*— Due to the rapid adoption of power electronics technology in shipboard microgrids (SMGs) in recent years, harmonic contamination has become now a crucial topic for these power systems. In order to sustain the safety of the electrical power systems, standards for power quality have imposed strict limits on the harmonic distortion allowed. In these standards, the application of the fast Fourier transform (FFT) with a window size of 10/12 cycles is often recommended for the harmonic evaluation. This method is not practical for SMGs due to large variations in load and frequency in a short duration. To address this issue, this article proposes a signal periodicity-independent algorithm to estimate the current harmonic distortion of SMGs by solving an eigenvalue problem with a short transient response. The proposed algorithm, which is based on a resolution-enhanced sliding matrix pencil method (SMPM), is distinguished by its frequency independency feature, and as a result of this, feature system frequency variations and the existence of interharmonics do not affect its accuracy. The evaluation of the proposed method is carried out under the MATLAB software and is experimentally verified via analyzing the electrical power system current of a container ship.**

***Index Terms*— Frequency estimation, harmonics distortion assessment, power quality, shipboard microgrids (SMGs).**

I. Introduction

IN RECENT years, shipboard microgrids (SMGs) have experienced a significant revolution by moving toward all-electrical SMGs through the installation of power electronics converters (PECs) [1], [2]. This advancement provides numerous advantages, such as easier maneuverability, speed and controllability of the power flow, saving space, and decreasing fuel consumption. However, the application of variable voltage/frequency drives causes considerable harmonics contamination to the electrical power system [3], [4]. An accurate assessment of harmonics can provide substantial information about the dangers of the circulation of these harmonics and, thus, enables engineers to verify whether these harmonic distortions comply with the most widely accepted standards or requires interfering to mitigate them. There are several classifications standards for ships and rules that deal with power quality issues [5]. These classification standards are very similar to the most often cited IEC standards 61000-4-7/30 [6], [7] and the underrevised IEEE 519 standards [8]. However, these standards include some recommendations, mainly regarding the existence of the interharmonics, that are not suitable for SMGs such as [5], [9] the following.

1) Use of the discrete Fourier transform (DFT) to analyze the harmonics.
2) The window width of the analyzed data should be 12 cycles of the fundamental frequency in case the fundamental frequency is 60 Hz.
3) Harmonic values are assessed and aggregated over three time intervals (3-s interval, 10-min interval, and 2-h interval).

The DFT is a frequency-dependent technique, which requires a bandwidth that corresponds to the fundamental frequency. Therefore, if the periodicity of the DFT data set does not fit the periodicity of the fundamental because of frequency drift, it results in spectral leakage and the picket fence effect. Moreover, the existence of the harmonics that are not integer multiples of the fundamental frequency disturbs its performance. In this respect, the aforementioned standards require aggregation of consecutive 12-cycle time intervals for a 60-Hz power system. However, since the DFT can only operate in the steady-state condition, a window width of 12 cycles of a steady-state signal is not practical for SMGs due to the large variation in the frequency and load in a short duration. In addition, a spectral resolution of 5 Hz is not accurate enough to reflect practically interharmonic locations [9]. As a result, following the standards, recommendations are most likely not very practical for SMGs. Addressing this

Manuscript received February 19, 2020; revised May 3, 2020, June 21, 2020, and August 3, 2020; accepted August 20, 2020. Date of publication September 1, 2020; date of current version September 18, 2020. This work was supported by VILLUM FONDEN under the VILLUM Investigator under Grant 25920 [Center for Research on Microgrids (CROM)]. The work of Chun-Lien Su was supported by the Ministry of Science and Technology of Taiwan under Grant MOST 107-2221-E-992-073-MY3. *(Corresponding author: Chun-Lien Su.)*

Yacine Terriche, Muhammad Umair Mutarraf, Josep M. Guerrero, Juan C. Vasquez, and Saeed Golestan are with the Department of Energy Technology, Aalborg University, 9220 Aalborg, Denmark (e-mail: yte@et.aau.dk; mmu@et.aau.dk; joz@et.aau.dk; juq@et.aau.dk; sgd@et.aau.dk).

Abderrzak Laib is with the Department of Electrical Engineering, University of Jijel, Jijel 18000, Algeria (e-mail: abderrzaklaib@yahoo.fr).

Chun-Lien Su is with the Department of Electrical Engineering, National Kaohsiung University of Science and Technology, Kaohsiung City 80778, Taiwan (e-mail: cls@nkust.edu.tw).

Digital Object Identifier 10.1109/TTE.2020.3020820

problem, several techniques that can estimate the harmonics and interharmonics in a short duration have been proposed in the existing literature. Wavelet packet decomposition [10], adaptive estimation of the fundamental-based-technique [11], least-squares (LS) technique [12], [13], Kalman filter [14], and ADALINE artificial neural networks [15] are some examples of such approaches. None of these techniques, however, have claimed to perform effectively in interharmonic assessment with system frequency drifts although each technique does demonstrate its own particular advantages. A measurement technique based on recursive group-harmonic power minimizing has been presented in [16] to overcome the problem of DFT leakage phenomenon under frequency drifts. This technique, however, requires a large window width, which limits its effectiveness for SMGs for the reasons stated earlier. Other methods utilize the Prony technique to assess the interharmonics. The Prony method (PM), however, demands a considerable computational effort as it is a two-step estimation process [17]. In addition, the PM has been proven to be highly sensitive to noise [18]. The matrix pencil method (MPM) can overcome the deficiency of the frequency dependence characteristics and, hence, estimates the harmonics and interharmonics of a system under large frequency drifts [17], [18]. However, if a signal is measured with large sampling time (a small number of bins per cycle) and has high harmonic distortion, then the MPM fails to estimate all the eigenvalues that provide correct information about the phasors of the signal. For these reasons, this technique—MPM—has not received much attention to the estimation of the total harmonics distortion (THD). This issue, however, can be solved by increasing the window width of the analyzed data. Unfortunately, this solution slows down the transient response of the sliding window and causes large errors, particularly for SMGs due to the high variations of load and frequency in a short duration.

In order to overcome the abovementioned shortcoming of MPM, this article proposes a periodicity-independent algorithm based on sliding MPM (SMPM), which can improve the resolution of the MPM without changing the sampling time or increasing the bandwidth of the buffered data. The proposed algorithm can accurately estimate the harmonics/interharmonics in only a half cycle. Moreover, the SMPM estimates the frequencies of the buffered distorted signal in a sliding window and, concurrently, adapts the window width of the LS approach in accordance with the fundamental frequency. Consequently, the root mean square (rms) of each harmonic component is accurately estimated, which enables the precise estimation of the THD in a short moving window even under large frequency drifts. The performance of the proposed algorithm is first evaluated under the MATLAB software. Experimental validation is then provided via analyzing the data of the current of a mooring winch and windlass on a container ship.

The remainder of this article is organized as follows. Section II presents the background of measuring the harmonic distortion and explains the fast Fourier transform (FFT) leakage deficiency. Section III presents the proposed algorithm. In Section IV, the results of a simulation with some discussions are presented. In Section V, the experimental validation of the proposed method is provided, and Section VI concludes this article.

II. Background of the Harmonic Distortion Measurement and FFT Leakage Deficiency

A. Overview

Harmonic distortion evaluation is one of the crucial indices that define the level of distortion of any type of periodic signal. The most common appellation for this process is the THD [19]. The THD can be interpreted with several concepts. Based on the literature consensus, the most commonly used formula for the THD is expressed as [9], [19]

$$\mathrm{THD} = \frac{\sqrt{\sum_{h=2}^{n} Y_h^2}}{Y_1} \cdot 100 \tag{1}$$

where Y_1 and Y_h are, respectively, the rms values of the fundamental component and an h-order harmonic component. n is the number of harmonics, which is often selected to be equal to 40 or 50. International standards often employ the FFT algorithms for the THD estimation. The FFT benefits from some interesting features, such as the ease of implementation and the ability of estimating a large scale of poles. However, it is highly sensitive to the frequency drifts and interharmonics, which results in the spectral leakage and picket fence effect. To deal with this problem, the most commonly used standards, such as the IEC 61000-4-7/30 standards, provide different indexes of the THD calculated in different ways, such as the group total harmonic distortion (THDG) and the subgroup total harmonic distortion (THDS). However, since the spread of spectral energy caused by frequency drifts merges with interharmonics, it results in incorrect estimation. Therefore, these standards require a window length of 12 cycles to assess the THD to reduce the effect of the interharmonics and frequency drifts. In other standards covering electrical installations on SMG, such as IEEE Standard 45-2002 [20] and IEC Standard 60092-101:2002 [21], the THD is defined as $(Y_{\mathrm{rms}}^2 - Y_1^2)^{1/2}/Y_1$, where Y_{rms} is the true rms value of the distorted signal. This definition is sometimes referred to as total waveform distortion (TWD) [22], [23]. However, the existence of the interharmonics causes large fluctuations in calculating Y_{rms} and requires several cycles to damp.

B. Glimpse of the FFT Leakage Phenomena

The DFT is the most commonly used technique in different areas of analysis, such as harmonic filtering, spectral analysis, complexity minimization, and equalization. For any length-N complex input sequence $x(n)$ with all integers n ($x(n) = x_0, x_1, \ldots, x_{N-1}$), the DFT is expressed as [24]

$$X(k) = \sum_{n=0}^{N-1} x(n) W_N^{kn} = \sum_{n=0}^{N-1} x(n) \left[\cos\left(\frac{2\pi}{N} kn\right) - i \cdot \sin\left(\frac{2\pi}{N} kn\right)\right] \tag{2}$$

where $W_N = e^{-j2\pi/N}$, and $k = 0, \ldots, N-1$.

Using (2), the inverse DFT (IDFT) of (2) in the domain $n \in [0, N-1]$ is given by

$$x(n) = \frac{1}{N}\sum_{k=0}^{N-1} X(k) W_N^{-kn}, \quad n \in \mathbb{Z}. \tag{3}$$

The FFT is a method that operates the DFT in an effective way to achieve the same results with a calculation burden that is decreased from $O(N^2)$ to $O(N \log N)$[25]. According to (3), if we set the product $X(k)W_N^{-kn} = A$, then (3) matches the expression of the moving average filter (MAF), which is presented in the discrete domain as [13]

$$x(n) = \frac{1}{N}\sum_{k=0}^{N-1} A(k). \tag{4}$$

In the continuous-time domain, (4) is corresponding to

$$x(t) = \frac{1}{T_w}\int_{t-T_w}^{t} X(\tau) d\tau \tag{5}$$

where T_w is the window length. In the Laplace domain, the MAF transfer function is presented as [26]

$$\mathrm{MAF}_{\mathrm{con}}(s) = \frac{x(s)}{A(s)} = \frac{1 - e^{-T_w s}}{T_w s}. \tag{6}$$

According to the Padé approximation, $e^{-T_w s}$ can be approximated as

$$e^{(-T_w s)} = e^{\left(-\frac{1}{2}T_w s\right)} / e^{\left(\frac{1}{2}T_w s\right)} = (1 - T_w s/2)/(1 + T_w s/2). \tag{7}$$

Substituting (7) into (6) results in

$$\mathrm{MAF}_{\mathrm{con}}(s) \approx 1/(1 + (0.5 T_w s)). \tag{8}$$

The transfer function (8) demonstrates that the DFT/MAF can function as an ideal low-pass filter when its window length is an integer multiple of the fundamental ($T_w = 1/\mathrm{nf}$).

A clear vision of the weakness of the DFT/MAF can also be proved in the following manner; if we substitute $s = j\omega$ into (6), it results in:

$$\mathrm{MAF}_{\mathrm{con}}(j\omega) = \frac{1}{T_w j\omega} - \frac{\cos(-T_w\omega) + j\sin(-T_w\omega)}{T_w j\omega}. \tag{9}$$

From (9), it is clear that if $T_w = 1/f$ or very close to it, (i.e., $f = 60$ Hz and $T_w = 0.0166$), then their multiplication in (9) provides a unity gain $f \cdot T_w \approx 1$; thus, (9) tends to zero ($\mathrm{MAF}_{\mathrm{con}}(j\omega) \approx 0$). This demonstration is visualized in Fig. 1 where it is clear that the MAF/DFT can provide a zero gain only at the sections where $f \cdot T_w \approx 1$. Any deviation from the unity of the product $f \cdot T_w$ results in decreasing the accuracy of the filter and, consequently, causes the spectral leakage.

III. Proposed SMPM Algorithm

The MPM is a polynomial developed technique arising from the PM, which has demonstrated its effectiveness in solving the problem of functions' interpolation based on an integral summation of exponentials [27]. The singular value decomposition (SVD) has been incorporated into the MPM to strengthen its immunity against noisy signals [28], [29]. A performance comparison between the MPM and PM has been evaluated in [28], where the authors proved that the

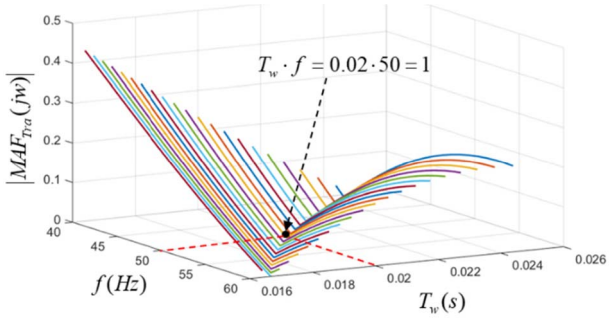

Fig. 1. Amplitude error of the MAF causes by the mismatches of the fundamental frequency and the bandwidth of the filter.

MPM provided a faster transient response with less sensitivity to noise. Another feature that distinguishes the MPM from its counterparts is the efficient computation burden since the MPM applies the one-step process, while the PM needs a two-step process to estimates the exponential of each frequency [17].

Based on the PM method, any distorted signal can be approximated by a sum of exponentials $e^{(-\alpha_i + j\omega_i)t}$ and residues $\Re_i$ as

$$Y(t) \approx \sum_{i=1}^{M} \Re_i e^{(-\alpha_i + j\omega_i)t} + \eta(t) \tag{10}$$

where α_i and ω_i represent, respectively, the damping factor and the angular frequency for each pole i, and $\eta(t)$ is the noise resulted from the measurement. M is the tolerance that selects the number of the aimed frequencies for $i = 1, 2, \ldots, M$. Since the recorded signals are not continuous and contain a limited number of samples γ, the discretization of (10) with the sampling time T_s is formulated as

$$Y(kT_s) \approx \sum_{i=1}^{M} \Re_i e^{(-\alpha_i + j\omega_i)kT_s} + \eta(kT_s). \tag{11}$$

The implementation of the MPM starts by choosing a random number of samples Υ, which corresponds to at least a cycle or a half cycle of the fundamental frequency f plus the maximum frequency deviation $\Delta f_{\max}$ that can occur to the power source depending on the sampling time as

$$\Upsilon \geq \frac{1}{c \cdot (f + |\Delta f_{\max}|) \cdot T_s}, \qquad \begin{array}{l} c = 1 \text{ if } T_s > 5e^{-4} \\ c = 1/2 \text{ if } T_s \leq 5e^{-4}. \end{array} \tag{12}$$

Contrary to the most common techniques that are applied in signal processing, such as the FFT, the MPM is featured by the ability to estimate the phasors of the harmonics in only a half cycle, even in the existence of interharmonics. The selection of Υ enables building the Hankel matrix $[A]$, where every descending skew-diagonal from the right side to the left is fixed

$$[A] = \begin{bmatrix} a(1) & a(2) & \ldots & a(L+1) \\ a(2) & a(3) & \ldots & a(L+2) \\ \vdots & \vdots & \ddots & \vdots \\ a(\gamma - L) & a(\gamma - L + 1) & \ldots & a(\gamma) \end{bmatrix}_{(\gamma - L)(L+1)}. \tag{13}$$

The parameter L is known as the pencil parameter [30]. In order to enhance the noise immunity of the MPM, L can be selected in the following range $(\gamma/3) \leq L \leq (\gamma/2)$ [31], [32]. The next process is to operate the SVD, which factorizes (13) into three matrices that estimate the variations (frequencies) of the input data and rearrange the frequencies in descending order as

$$[A] = [U]\left[\sum\right][V]^* \tag{14}$$

$$[U] = \begin{bmatrix} u_{1,1} & u_{1,2} & \dots & u_{1,\gamma-L} \\ u_{2,1} & u_{2,2} & \dots & u_{2,\gamma-L} \\ \vdots & \vdots & \ddots & \vdots \\ u_{\gamma-L,1} & u_{\gamma-L,2} & \dots & u_{\gamma-L,\gamma-L} \end{bmatrix}_{(\gamma-L)(\gamma-L)} \tag{15}$$

$$\left[\sum\right] = \begin{bmatrix} \sigma_1 & 0 & \dots & 0 \\ 0 & \sigma_2 & \dots & 0 \\ \vdots & \vdots & \ddots & \vdots \\ 0 & 0 & \dots & \sigma_\gamma \end{bmatrix}_{(\gamma-L)(L+1)} \tag{16}$$

$$[V] = \begin{bmatrix} u_{1,1} & u_{1,2} & \dots & u_{1,L+1} \\ u_{2,1} & u_{2,2} & \dots & u_{2,L+1} \\ \vdots & \vdots & \ddots & \vdots \\ u_{L+1,1} & u_{L+1,2} & \dots & u_{L+1,L+1} \end{bmatrix}_{(L+1)(L+1)} \tag{17}$$

where $*$ denotes the transpose of the matrix. $[U]$ and $[V]$ are, respectively, the left and right singular vectors of $[A]$ that comprises, respectively, the orthonormal eigenvectors of $[A] \cdot [A]^*$ and $[A]^* \cdot [A]$. $[\sum]$ consists of the square roots of the nonnegative eigenvalues σ_i that are usually called the singular values of the products $[A] \cdot [A]^*$ and $[A]^* \cdot [A]$. Usually, for undamped signals, σ_i appears as pair values; hence, each pair represents a certain frequency. For example, if we select M to the first two singular values, the algorithm will estimate the fundamental frequency. However, the main deficiency of the MPM is the limitation of the number of harmonics Nh that is constrained to the parameter L and can be defined as

$$Nh = \frac{\sigma_{2L+2}}{2} = \frac{L+1}{2}, \quad \frac{\gamma}{3} \leq L \leq \frac{\gamma}{2} \tag{18}$$

where σ_{2L+2} denotes the maximum number of the singular values. If we select $L = \gamma/2$, then the number of harmonics that can be estimated using the traditional MPM is $Nh = \gamma/4$. Since L is proportional to Υ, and Υ is constrained to T_s, it implies that the number of frequencies extracted by the MPM is inversely proportional to T_s. Furthermore, based on the Nyquist criterion, if the harmonics that exist in the buffered signal are over the folding frequency $f_{\max}(Hz)$ ($f_{\max} = 1/(2T_s)$), aliasing will increase once the signal is buffered. Hence, all the singular values that have a larger rank than $\sigma_{\max}$, which corresponds to $f_{\max}(Hz)$, are essentially noise that causes misinformation about the actual harmonics of that rank.

In order to avoid the deficiencies of traditional MPM, this article proposes a method to enhance the resolution of the MPM by fitting the Hankel matrix. The procedure starts by

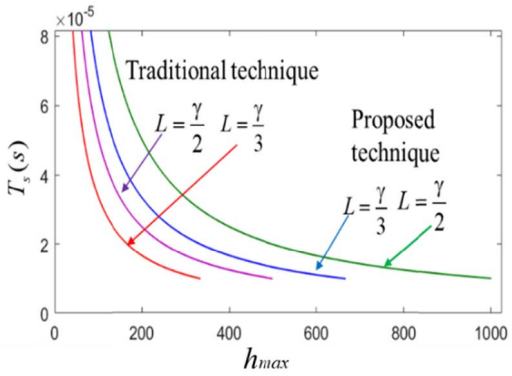

Fig. 2. Maximum number of harmonics that can be assessed using the MPM with different values of L.

defining two matrices extracted from the Hankel matrix as

$$[A_a] = \begin{bmatrix} a(2) & a(3) & \dots & a(L+2) \\ a(3) & a(4) & \dots & a(L+3) \\ \vdots & \vdots & \ddots & \vdots \\ a(\gamma-L) & a(\gamma-L+1) & \dots & a(\gamma) \end{bmatrix}_{(\gamma-L-1)(L+1)} \tag{19}$$

$$[A_b] = \begin{bmatrix} a(1) & a(2) & \dots & a(L+1) \\ a(2) & a(3) & \dots & a(L+2) \\ \vdots & \vdots & \ddots & \vdots \\ a(\gamma-L-1) & a(\gamma-L) & \dots & a(\gamma-1) \end{bmatrix}_{(\gamma-L-1)(L+1)} \tag{20}$$

where $[A_a]$ and $[A_b]$ are, respectively, obtained by removing the first and last rows of the Hankel matrix $[A]$. Then, the next step is to sum up these two matrices and divide them by 2 to obtain the fit value of each two values for every row of the Hankel matrix as

$$[A_C] = \frac{[A_a] + [A_b]}{2}. \tag{21}$$

Finally, the novel Hankel matrix is built by alternating rows/columns from $[A_c]$ and $[A]$ to produce the fit Hankel Matrix that is presented in (22) at the bottom of the next page.

Fig. 2 portrays the maximum number of harmonics that are estimated by the traditional MPM and the proposed method in terms of T_s and L. It is clear that selecting different values of T_s and L results in estimating a different number of harmonics. Therefore, the existence of the interharmonics leads to the saturation of $f_{\max}$. Consequently, the matrix cannot provide sufficient information on all existent singular values of each harmonic, which leads to inaccurate THD. However, the proposed method can provide the double number of the singular values for each value of the parameter L. Consequently, the algorithm will be able to extract the double number of the harmonics and, therefore, a more accurate THD calculation. After selecting the desired number of harmonics, the inverse SVD cannot be performed due to the unfit size of the matrices. Hence, $[V]$ is reduced into two submatrices as

$$[V_a] = \left[V(1 : \gamma - L - 1, 1 : M)\right] \tag{23}$$

$$[V_b] = \left[V(2 : \gamma - L, 1 : M)\right]. \tag{24}$$

The matrices $[V_a]$ and $[V_b]$ are attained by deleting the last and first rows of $[V]$, respectively, thus resulting in the following two matrices:

$$[A_1] = [U]\left[\sum\right][V_a]^* \tag{25}$$

$$[A_2] = [U]\left[\sum\right][V_b]^*. \tag{26}$$

As the reduction of $[V]$ into $[V_a]$ and $[V_b]$ results in the two matrices $[A_1]$ and $[A_2]$, the estimation of the frequencies of the distorted signal can be solved as $[A_2] - \lambda[A_1]$ that can be shortened to $[A_1]^+[A_2] - \lambda[I]$, where $[I]$ is referred to as the identity matrix, λ is the eigenvalue, and $+$ denotes the Moore–Penrose pseudoinverse [18]. The MPM estimates the eigenvalues λ_i as a pair complex number, where each pair corresponds to one frequency that is estimated as

$$f_i = \text{imag}(\log(\lambda_i))/(2\pi T_s), \quad i = 1, 2, \ldots, M. \tag{27}$$

After the estimation of each exponential using (27), the amplitude of each exponential is determined by implementing the least-squares technique as [13]

$$\begin{bmatrix} y(1) \\ y(2) \\ \vdots \\ y(\gamma) \end{bmatrix} = \begin{bmatrix} 1 & 1 & \cdots & 1 \\ \partial_1 & \partial_2 & \cdots & \partial_M \\ \vdots & \vdots & \ddots & \vdots \\ \partial_1^{\gamma-1} & \partial_2^{\gamma-1} & \cdots & \partial_M^{\gamma-1} \end{bmatrix} \begin{bmatrix} \Re_1 \\ \Re_2 \\ \vdots \\ \Re_M \end{bmatrix} \tag{28}$$

where $\partial_i = e^{(-\alpha_i + j\omega_i)T_s}$. The purpose of this hypothesis is to obtain $\Re_i$ with the best approximation. Hence, the least-squares equation becomes

$$\begin{bmatrix} \Re_1 \\ \Re_2 \\ \vdots \\ \Re_M \end{bmatrix} = \begin{bmatrix} y(1) \\ y(2) \\ \vdots \\ y(\gamma) \end{bmatrix} \backslash \begin{bmatrix} 1 & 1 & \cdots & 1 \\ \partial_1 & \partial_2 & \cdots & \partial_M \\ \vdots & \vdots & \ddots & \vdots \\ \partial_1^{\gamma-1} & \partial_2^{\gamma-1} & \cdots & \partial_M^{\gamma-1} \end{bmatrix}. \tag{29}$$

Fig. 3(a) presents the proposed SMPM that contains two short moving windows. The size γ of the first moving window $\psi(k)$ is fixed and selected to a half or one cycle plus $\Delta f_{\max}$, as explained in (11). If we ignore the noise, then the sliding window of the proposed method can be formulated as

$$A(kT_s) \approx \sum_{m=1}^{M} \sum_{i=1}^{M} \Re_i \cdot \Im^{kT_s} \psi\left(k - m\frac{\gamma}{y}\right), \quad m\frac{\gamma}{y} \in [1, P] \tag{30}$$

where $\Im = e^{(-\alpha_i + j\omega_i)}$. P is the size of the fully analyzed data. m is the desired number of windows of A. y refers to the overlapping between the windows. In real applications, such as the variation of the operation modes of the ships, the value and the frequencies of the signal change over time. Thus, it is more logical to select a short moving window $\psi(k)$ of the proposed method, which considers the frequency variation over time. In order to provide better clarification of this concept, an example of a moving window with three values of the fracture m/y is presented in Fig. 3(b), where γ is set to 12 samples. In the case of an accurate estimation of the frequencies, the overlapping between the windows can be selected for each sample. However, to clearly visualize the frequency variation over time and reduce the computational burden particularly for long streams of data, the shift between the windows can be selected to one cycle. Once the frequencies of each sampling window are defined, the proposed algorithm detects whether the signal contains interharmonics or not. This procedure can be easily implemented in MATLAB/programming software for each estimated frequency as

$$f_{\text{inter}}(i) = |f_i - \text{round}(f_i)|, \quad f_i \in \mathbb{Z}^+, \ \text{round}(f_i) \in \mathbb{N}^+. \tag{31}$$

The function round(f_i) removes all the digits after the comma and approximates f_i to the closer natural value. Then, if $f_{\text{inter}}(i) > 0 + \text{erro}$, it implies that the interharmonics exist, where the term erro denotes the error that can occur during the measurement and calculation. In this article, to achieve a satisfactory compromise between accuracy and the number of the estimated exponentials, erro $= 0.1$ is selected. After separating the harmonics and interharmonics, the algorithm gives engineers the choice of either calculating the THD of harmonics and the THD of interharmonics individually or using a global THD using both harmonics and interharmonics as presented in this article.

IV. Numerical Results and Discussion

Numerical results were obtained using the MATLAB software. Fig. 4 presents the performance of the FFT with a short window, FFT recommended by the IEC standards, the traditional MPM, and the proposed method in this article. The selection of the standard FFT aims to demonstrate that this method, which is recommended by the most commonly used power quality standards, has weaknesses under some conditions, such as slow response during load variations. Furthermore, the traditional MPM is selected to prove that this method can overcome the weakness of the standard FFT. However, under poor sampling time conditions, its performance tends to worsen. Finally, our goal is to demonstrate that the proposed method can overcome the deficiencies of these

$$[A_e] = \begin{bmatrix} a(1) & \frac{a(1)+a(2)}{2} & \cdots & a(L+1) \\ \frac{a(1)+a(2)}{2} & a(2) & \cdots & \frac{a(L+1)+a(L+2)}{2} \\ a(2) & \frac{a(2)+a(3)}{2} & \cdots & a(L+2) \\ \vdots & \vdots & \ddots & \vdots \\ a(\gamma - L) & \frac{a(\gamma - L)+a(\gamma - L+1)}{2} & \cdots & a(\gamma) \end{bmatrix}_{(2\gamma - 2L - 1)(2L+1)} \tag{22}$$

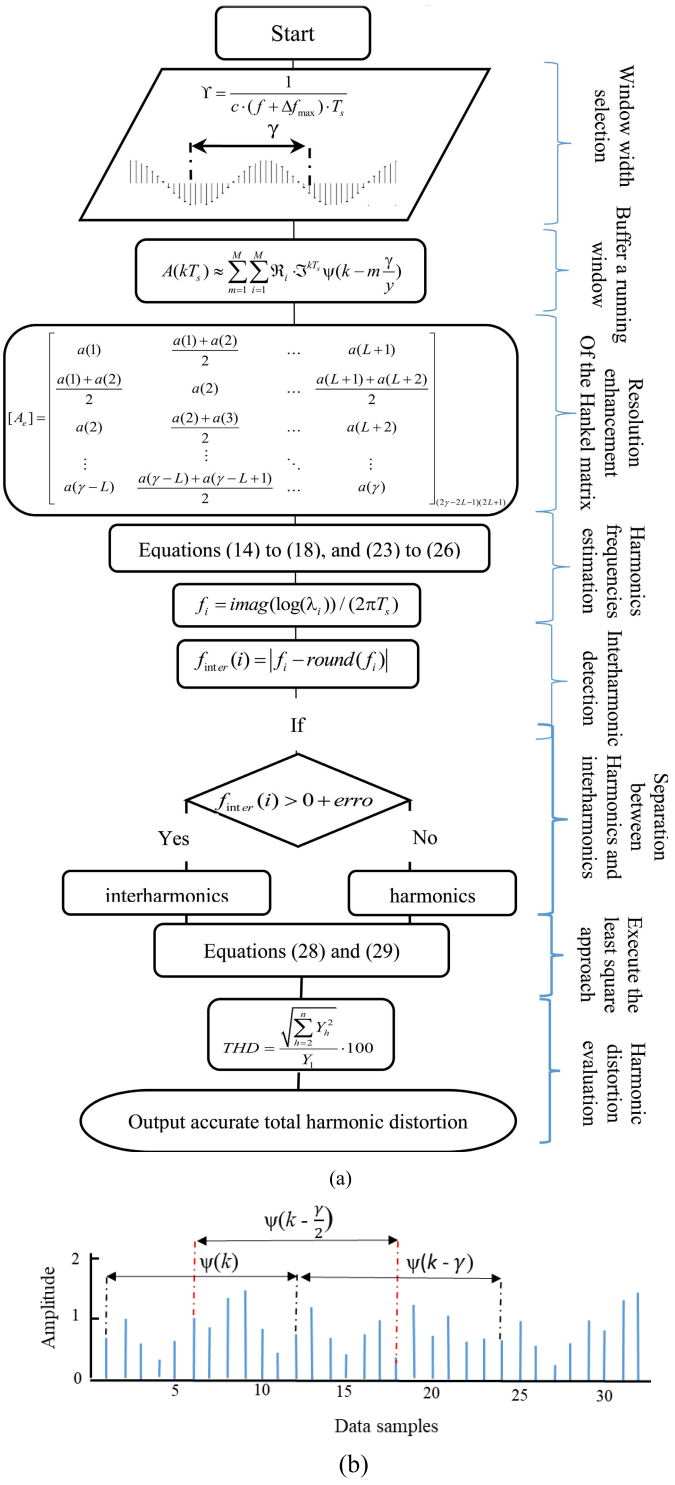

Fig. 3. (a) Flowchart of the proposed SMPM. (b) Window $\psi(k)$ of length $N = 12$ with three shifts of the fracture m/y (0, 1/2, 1).

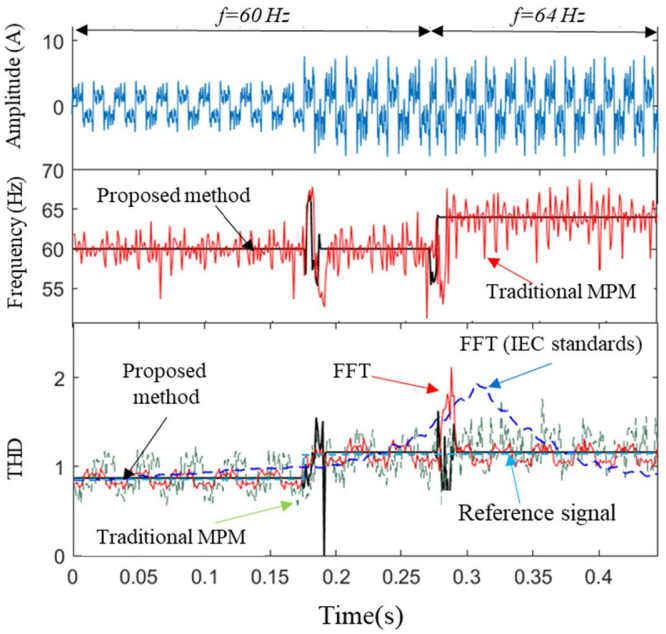

Fig. 4. Performance of the traditional MPM, FFT, FFT recommended by IEC standards, and the proposed method in estimating the THD under frequency and load variation.

traditional methods. In the study case, the frequency of the signal is set to 60 Hz, which then changes to 64 Hz in a period 0.27 s, and the amplitude of the signal changes in a period 0.16 s. The first subplot portrays the signal that is contaminated with the harmonic components of the frequencies 180, 300, 330, 420, 570, 660, 780, and 900 Hz and some Gaussian noise. The sampling time is set to $T_s = 1e^{-4}$ s. The middle plot displays the fundamental frequency that can only be estimated by the traditional MPM, and the proposed method here due to the fact that FFT cannot estimate the system frequency. Since the number of harmonics on the signal exceeds *Nh* [see (18)], it is shown clearly that traditional MPM fails to estimate the fundamental frequency. However, based on the enhanced resolution in the proposed method, the fundamental frequency is accurately estimated. Moreover, the dynamic response of the proposed method under variation of frequency and amplitude is very fast (half cycle). Furthermore, in the bottom plot, it is shown that the performance of FFT with a short window width (one cycle) tends to worsen when estimating the THD due to the existence of the interharmonics and frequency drifts, both of which adversely affect FFT performance. Finally, it is clear that the accuracy of the traditional MPM degrades due to the low resolution. Though the FFT recommended by IEC standards can overcome the oscillations caused by frequency drifts and interharmonics, it requires, however, a large transient response under frequency and load variations that lead to incorrect results. Since the proposed method can accurately estimate the frequencies of theexisting harmonics and interharmonics, it adapts the window width of the LS approach to these frequencies resulting in an accurate THD estimation and faster transient response (half cycle).

Fig. 5 presents the 3-D harmonic spectrums estimated, respectively, by the FFT with a short window [see Fig. 5(a)], FFT recommended by the IEC standards [see Fig. 5(b)], the traditional MPM [see Fig. 5(c)], and the proposed method [see Fig. 5(d)]. According to Fig. 5(a), it is clear that before the frequency drifts, the FFT causes a small leakage and picket fence effect due to the existence of the interharmonics. However, when the frequency drifts to 64 Hz, the spectral leakage increases resulting in incorrect values of each of the components. On the other hand, the FFT recommended by the

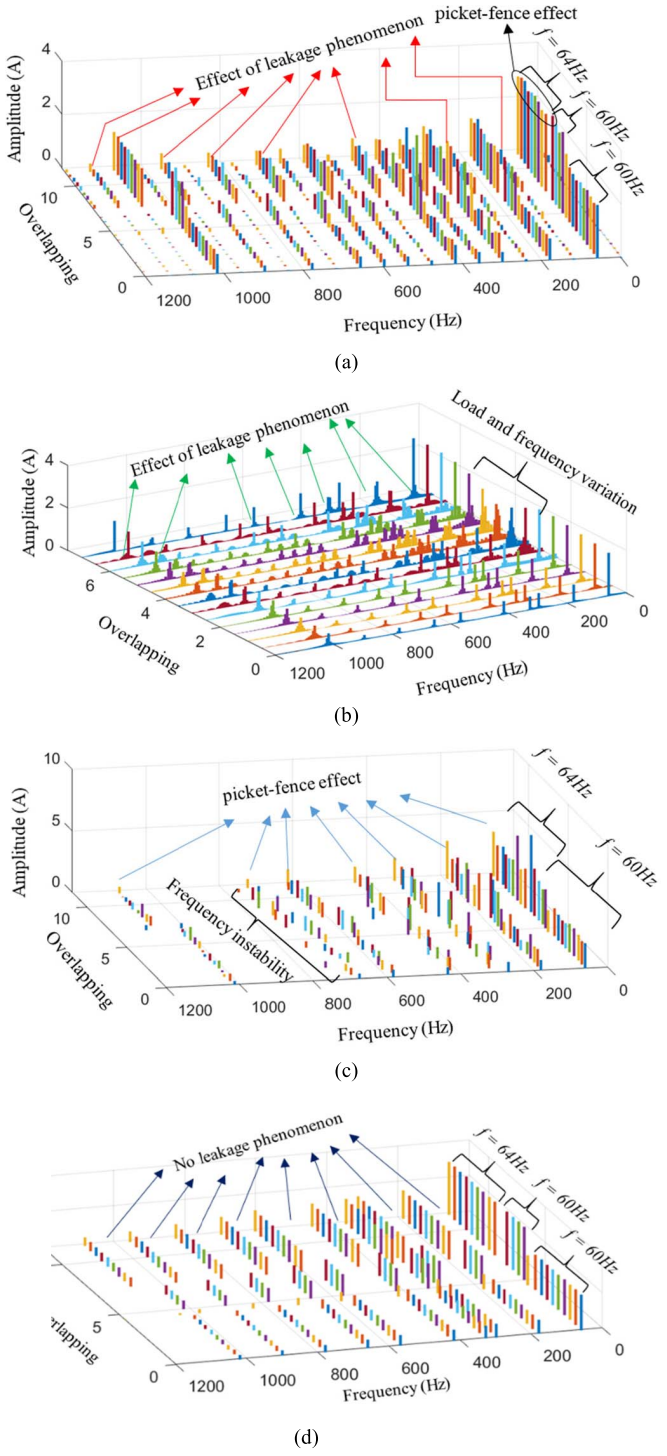

Fig. 5. 3-D harmonics spectrum estimated by (a) FFT with short window width, (b) FFT recommended by IEC standards, (c) traditional MPM, and (d) proposed method.

IEC standards provides a fixed amplitude of the fundamental frequency for each overlap. However, under frequency and amplitude variation, that requires a long transient response. Moreover, although the window width of 12 cycles decreases spectral leakage when the frequency is 60 Hz, it fails, however, to minimize the leakage when the frequency drifts to 64 Hz. According to Fig. 5(c), it is evident that the traditional MPM

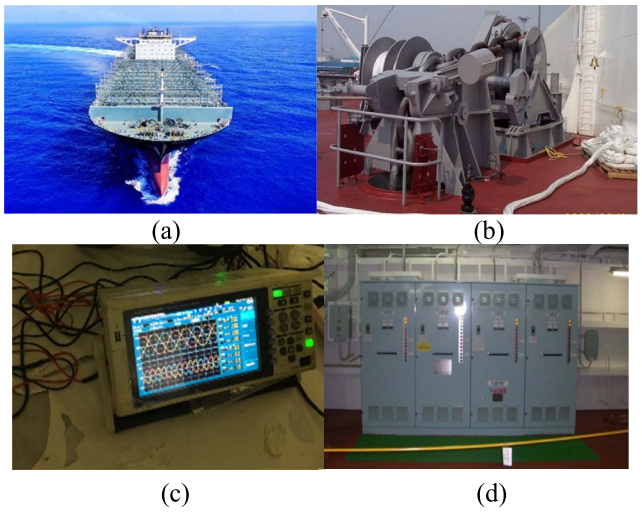

Fig. 6. Experimental measurements. (a) Photograph of the nominated container ship. (b) Windlass and mooring winch. (c) Measurement devices (Hioki 8847 Memory HiCorder). (d) Sensors of the measurement devices connected to the main switchboard of the electrical power system.

does not have problems of leakage phenomenon. However, as the number of harmonics on the signal exceeds *Nh,* the performance of this method is greatly affected resulting in incorrect harmonics and the picket fence effect. However, citing Fig. 5(d), we show that the proposed method can accurately estimate the harmonics and interharmonics without any spectral leakage phenomenon or picket fence effect. Moreover, the variation in the frequency and the amplitude does not affect the accuracy of the proposed method.

V. Experimental Analysis: Comparisons and Discussion

The validation of the proposed method was carried out via the analysis of the electrical power system current of a container ship that is shown in Fig. 6(a). Since this type of vessel is designed to hold large quantities of cargo compacted in different types of containers, the data are measured during the operation of the windlass and the mooring winches and are displayed in Fig. 6(b). The measurement device that is applied to collect the data is Hioki 8847 Memory HiCorder [see Fig. 6(c)]. The variable frequency drives that are applied to control the speed of the windlass and mooring winches are presented in Fig. 6(d). The main parameters of the electrical power system of the container ship are summarized in Table I.

Fig. 7 presents the performance of the proposed algorithm to evaluate the harmonics of the current under observation. The upper plot presents a distorted current. The second plot shows the capability of the proposed method in estimating the frequency of the fundamental frequency. The third subplot presents the capability of the proposed algorithm and the FFT suggested by the IEC standards in estimating the THD of the distorted current. The last plot presents the half symmetry of the current of the first subplot. According to the second plot, it is clear that the proposed algorithm can estimate the fundamental frequency of the system. The small ripples that appear on the frequency are due to the fact that, in real

TABLE I
PARAMETERS OF THE CONTAINER SHIP ELECTRICAL SYSTEM

Items and Equipment	Parameters	Values
Main AC bus voltage	Vabc[Vrms]	440 V
	f [Hz]	60 Hz
Diesel generator (3sets)	Vg[Vrms]	450 V
	Pg[kW]	1900 kW
	Xd'[%]	24.6
	Xd''[%]	17.2
	Cos(ψg)	0.8
Windlass & mooring winch (8 sets)	Vm[Vrms]	440 V
	Pm[kW]	45 kW
Main engine	Pm[kW]	20500 kW
Fuel tank	Weight[t]	202 tons
Speed	Knots	21 Knots

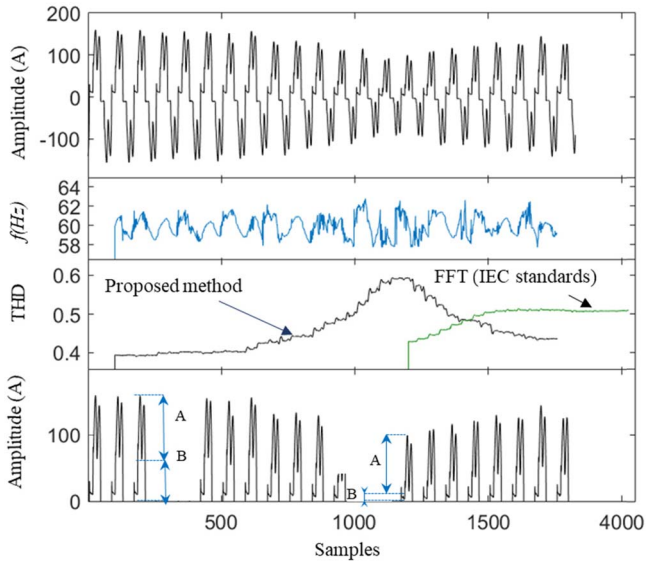

Fig. 7. Experimental validation of the proposed method and FFT for estimating the THD.

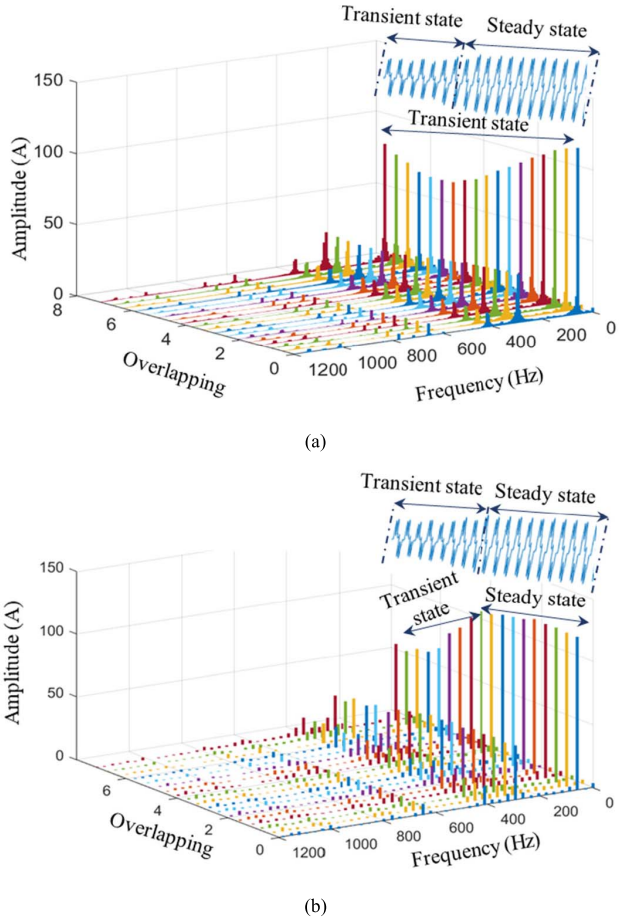

Fig. 8. Experimental spectral analysis using (a) FFT recommended by the IEC standards (b) SMPM.

applications, the frequency of the SMGs is not stable and varies rapidly for short durations and, therefore, estimating their frequency in a short moving window using sophisticated methods, such as the proposed algorithm in this article, is necessary. Moreover, the common techniques recommended by the standards, such as the FFT, are a frequency-dependent technique that cannot estimate the frequency in an open-loop pattern. In fact, they require precise information on the fundamental frequency to work properly. Turning out attention to the third Fig. 7, it is obvious that the proposed method provides an accurate estimation of the THD with a faster transient response that follows the variation of the current, which occurs after 600 samples. The small ripples that appear on the signal exist due to the large frequency variation of the SMGs, as mentioned earlier. Though the FFT recommended by the IEC standard provides fewer ripples, its dynamic response is very slow, which consequently causes incorrect estimation of the instantaneous THD for each sample. Even so, by viewing the last plot, it is evident that the length (A) of the notch is much bigger than the length (B) when the signal varies. This increase in notches results in more distortion. Therefore, the dynamic behavior of the proposed method matches the signal variation.

In order to confirm the performance of the proposed algorithm, Fig. 8 is presented. It displays the harmonic spectrum extracted by the FFT recommended by the IEC standards, while the results shown in Fig. 8(b) are obtained by the proposed method. The window overlap of the proposed algorithm is set to one sample, while the spectrum is depicted every one cycle to provide better visualization. Although the analyzed data have a steady-state condition of about 600 samples and transient state for the rest samples, the spectrum extracted by the FFT recommended by the IEC contains a transient state for the total analyzed data due to the large dynamic response of this method resulting in magnitude misinformation and spectral leakage. However, the spectrum estimated by the proposed algorithm presents fixed values during the steady state and then varies according to the signal variation; hence, it results in accurate values with a faster dynamic response. Traditional MPM and FFT with a short window are not added to the experimental part comparison due to the limitation of the number pages of the journal, as well as due to their low performance in the simulation section where the study was ideal.

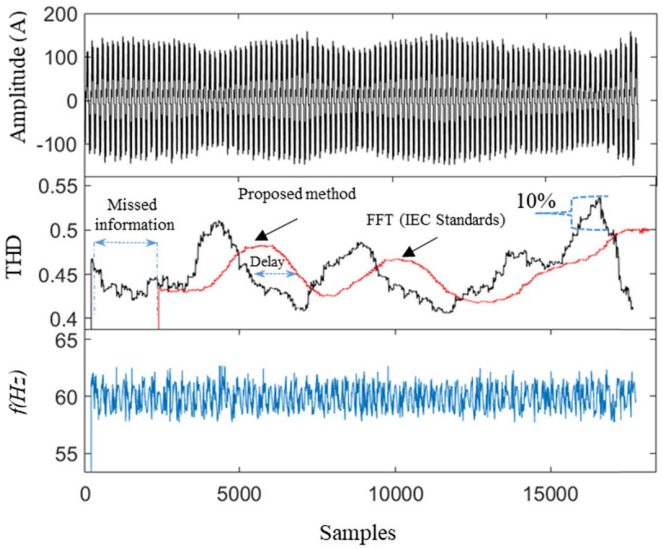

Fig. 9. Experimental performance comparisons of the proposed method with the standard FFT under a distorted nonstationary signal of a large data.

Fig. 9 is presented to demonstrate the performance of the proposed algorithm in analyzing a large set of data of the current analyzed in the experiment. The first subplot depicts the analyzed distorted current. The second subplot portrays the THDs estimated by the proposed method and the standard FFT. According to this subplot, it is evident that the THD measured by the standard FFT suffers from a large delay due to the wide moving window; hence, it cannot provide precise information on short-term disturbances. However, due to the short window size of the proposed method, the measured THD follows the small and large-term harmonic disturbances accurately. This can be seen in the overshoots that are estimated by the proposed method, while the standard FFT cannot estimate these overshoots due to large window width. Moreover, in contradiction with the FFT that cannot estimate the system frequency, the proposed method is featured by the ability to estimate the fundamental frequency, as presented in the last subplot of Fig. 9, where it shows that the frequency of the experimental data has large variations in a short time. Hence, the techniques that are frequency-dependent, such as the FFT, are not suitable for SMGs. Therefore, the proposed method is foreseen to be an effective tool for engineers to study the shipboard harmonics problem.

VI. Conclusion

In this article, a signal periodicity-independent algorithm has been proposed to estimate the THD of SMGs by solving the eigenvalue problem. The proposed algorithm is based on a resolution-enhanced SMPM that can estimate the harmonics and interharmonics in a short duration (half to one cycle) under large frequency drifts. The performance of the proposed algorithm is evaluated using the MATLAB software, and then, the experimental validation was provided by analyzing the data of the current of the mooring winches and the windlass on a container ship. According to the studies conducted, it was proven if the number of the harmonics of the contaminated signal is more than the double number of the eigenvalues that are estimated by the traditional MPM, then the MPM fails to provide an accurate estimation. However, based on the fit Hankel matrix, the resolution of the proposed SMPM is enhanced resulting in estimating the harmonics and interharmonic accurately and, hence, provides correct information of the THD. Furthermore, it has been verified that the FFT recommended by the power quality standards, such as the IEC standards and IEEE 519-2014, requires a large steady state (12 cycles for $f = 60$ Hz) to provide an accurate estimation, which is not practical for ships due to large load variation. Consequently, it results in an incorrect spectral assessment. Moreover, the FFT with a short window width fails to work properly in the existence of interharmonics or frequency drifts resulting in spectral leakage and the picket fence effect. Due to the short moving window of the SMPM and its periodicity independence characteristic, it has been demonstrated that the proposed algorithm can deal with the dynamic behavior of the loads effectively and results in accurate spectral analysis. As a result, this algorithm is foreseen to be very effective for SMGs data analysis.

References

[1] G. Sulligoi, A. Vicenzutti, and R. Menis, "All-electric ship design: From electrical propulsion to integrated electrical and electronic power systems," *IEEE Trans. Transport. Electrific.*, vol. 2, no. 4, pp. 507–521, Dec. 2016.

[2] X. Zhaoxia, Z. Tianli, L. Huaimin, J. M. Guerrero, C.-L. Su, and J. C. Vasquez, "Coordinated control of a hybrid-electric-ferry shipboard microgrid," *IEEE Trans. Transport. Electrific.*, vol. 5, no. 3, pp. 828–839, Sep. 2019.

[3] J. Mindykowski, "Power quality on ships: Today and tomorrow's challenges," in *Proc. Int. Conf. Expo. Electr. Power Eng. (EPE)*, Oct. 2014, pp. 1–18.

[4] Y. Terriche *et al.*, "A hybrid compensator configuration for VAR control and harmonic suppression in all-electric shipboard power systems," *IEEE Trans. Power Del.*, vol. 35, no. 3, pp. 1379–1389, Jun. 2020.

[5] J. Mindykowski, "Case study—Based overview of some contemporary challenges to power quality in ship systems," *Inventions*, vol. 1, no. 2, p. 12, Jun. 2016.

[6] *Electromagnetic Compatibility (EMC) Part 4-30: Testing and Measurement Techniques-Power Quality Measurements Methods*, Standard IEC 61000-4-30 Edition 2.0- 2008-10.

[7] *EMC _ Part 4-7: Testing and Measurements Techniques_General Guide on Harmonics and Interharmonics Measurements and Instrumentation, for Power Supply Systems and Equipment Connected Thereto*, Standard IEC 61000-4-7 Edition 2_2002-08.

[8] *Electromagnetic Compatibility (EMC) Part 4-30: Testing and Measurement Techniques-Power Quality Measurements Methods*, Standard IEC 61000-4-30, 2015.

[9] M. Aiello, A. Cataliotti, S. Favuzza, and G. Graditi, "Theoretical and experimental comparison of total harmonic distortion factors for the evaluation of harmonic and interharmonic pollution of grid-connected photovoltaic systems," *IEEE Trans. Power Del.*, vol. 21, no. 3, pp. 1390–1397, Jul. 2006.

[10] L. Eren, M. Unal, and M. J. Devaney, "Harmonic analysis via wavelet packet decomposition using special elliptic half-band filters," *IEEE Trans. Instrum. Meas.*, vol. 56, no. 6, pp. 2289–2293, Dec. 2007.

[11] D. M. McNamara, A. K. Ziarani, and T. H. Ortmeyer, "A new technique of measurement of nonstationary harmonics," *IEEE Trans. Power Del.*, vol. 22, no. 1, pp. 387–395, Jan. 2007.

[12] A. E. Zawawi, K. H. Youssef, and O. A. Sebakhy, "Recursive least squares harmonic identification in active power filters," in *Proc. Eur. Control Conf. (ECC)*, Jul. 2007, pp. 4645–4650.

[13] Y. Terriche, J. M. Guerrero, and J. C. Vasquez, "Performance improvement of shunt active power filter based on non-linear least-square approach," *Electr. Power Syst. Res.*, vol. 160, pp. 44–55, Jul. 2018.

[14] X. Nie, "Detection of grid voltage fundamental and harmonic components using Kalman filter based on dynamic tracking model," *IEEE Trans. Ind. Electron.*, vol. 67, no. 2, pp. 1191–1200, Feb. 2020.

[15] J. R. Salinas, F. Garcia-Lagos, J. D. de Aguilar, G. Joya, R. Lapuh, and F. Sandoval, "Harmonics and interharmonics spectral analysis by ANN," in *Proc. Conf. Precis. Electromagn. Meas. (CPEM)*, Ottawa, ON, Canada, Jul. 2016, pp. 1–2.
[16] H. C. Lin, "Power harmonics and interharmonics measurement using recursive group-harmonic power minimizing algorithm," *IEEE Trans. Ind. Electron.*, vol. 59, no. 2, pp. 1184–1193, Feb. 2012.
[17] K. Sheshyekani, G. Fallahi, M. Hamzeh, and M. Kheradmandi, "A general noise-resilient technique based on the matrix pencil method for the assessment of harmonics and interharmonics in power systems," *IEEE Trans. Power Del.*, vol. 32, no. 5, pp. 2179–2188, Oct. 2017.
[18] T. K. Sarkar and O. Pereira, "Using the matrix pencil method to estimate the parameters of a sum of complex exponentials," *IEEE Antennas Propag. Mag.*, vol. 37, no. 1, pp. 48–55, Feb. 1995.
[19] D. Shmilovitz, "On the definition of total harmonic distortion and its effect on measurement interpretation," *IEEE Trans. Power Del.*, vol. 20, no. 1, pp. 526–528, Jan. 2005.
[20] *IEEE Recommended Practice for Electric Installations on Shipboard*, IEEE Standard 45-2002 (Revision of IEEE Std 45-1998), Oct. 2002, pp. 1–272.
[21] *Electrical Installations in Ships. Definitions and General Requirement*, Standard IEC Standard 60092-101, 2002.
[22] T. Tarasiuk and J. Mindykowski, "An extended interpretation of THD concept in the wake of ship electric power systems research," *Measurement*, vol. 45, no. 2, pp. 207–212, Feb. 2012.
[23] M. H. J. Bollen and I. Y.-H. Gu, *Signal Processing of Power Quality Disturbances*. Piscataway, NJ, USA: IEEE, 2006.
[24] J. Borkowski, D. Kania, and J. Mroczka, "Interpolated-DFT-based fast and accurate frequency estimation for the control of power," *IEEE Trans. Ind. Electron.*, vol. 61, no. 12, pp. 7026–7034, Dec. 2014.
[25] S. M. Seo, "A fast IE-FFT algorithm to analyze electrically large planar microstrip antenna arrays," *IEEE Antennas Wireless Propag. Lett.*, vol. 17, no. 6, pp. 983–987, Jun. 2018.
[26] S. Golestan, J. M. Guerrero, and A. M. Abusorrah, "MAF-PLL with phase-lead compensator," *IEEE Trans. Ind. Electron.*, vol. 62, no. 6, pp. 3691–3695, Jun. 2015.
[27] R. Prony, "Essai expérimental et analytique, etc," *Paris J. l'Ecole Polytech. Floréal Plairial*, vol. 2, no. 22, pp. 24–76, 1795.
[28] Y. Hua and T. K. Sarkar, "Matrix pencil method for estimating parameters of exponentially damped/undamped sinusoids in noise," *IEEE Trans. Acoust., Speech, Signal Process.*, vol. 38, no. 5, pp. 814–824, May 1990.
[29] R. S. Adve, T. K. Sarkar, O. M. C. Pereira-Filho, and S. M. Rao, "Extrapolation of time-domain responses from three-dimensional conducting objects utilizing the matrix pencil technique," *IEEE Trans. Antennas Propag.*, vol. 45, no. 1, pp. 147–156, Jan. 1997.
[30] Y. Hua and T. K. Sarkar, "Generalized pencil-of-function method for extracting poles of an EM system from its transient response," *IEEE Trans. Antennas Propag.*, vol. 37, no. 2, pp. 229–234, Feb. 1989.
[31] Y. Hua and T. K. Sarkar, "On the total least squares linear prediction method for frequency estimation," *IEEE Trans. Acoust., Speech, Signal Process.*, vol. 38, no. 12, pp. 2186–2189, Dec. 1990.
[32] Y. Terriche, S. Golestan, J. M. Guerrero, D. Kerdoune, and J. C. Vasquez, "Matrix pencil method-based reference current generation for shunt active power filters," *IET Power Electron.*, vol. 11, no. 4, pp. 772–780, Apr. 2018.

Yacine Terriche received the B.S. degree in electrical engineering from the University of Science and Technology, Constantine, Algeria, in 2011, and the M.S. degree in electrical engineering from the University of Constantine 1, Constantine, in 2013. He is currently pursuing the Ph.D. degree with the Department of Energy Technology, Aalborg University, Aalborg, Denmark.

From December 2019 to September 2020, he was a Researcher Assistant with the National Kaohsiung University of Science and Technology, Kaohsiung, Taiwan. His research interests include power electronics, modeling, control, signal processing, power quality issues, active and passive power filters, and terrestrial and shipboard microgrids.

Muhammad Umair Mutarraf (Student Member, IEEE) received the B.Sc. degree in electrical engineering from the University of Engineering and Technology, Lahore, Pakistan, in 2013, and the M.Eng. degree in control theory and control engineering from Xidian University, Xi'an, China, in 2017. He is currently pursuing the Ph.D. degree with the Department of Energy Technology, Aalborg University, Aalborg, Denmark.

His research interests include power electronics, modeling, control, and integration of energy storage in ac and dc shipboard microgrids.

Abderrzak Laib received the master's degree in telecommunications engineering from the University of M'sila, M'sila, Algeria, in 2012, and the Ph.D. degree in electrical engineering from the University of Jijel, Jijel, Algeria, in 2018.

He is currently with the Department of Electrical Engineering, University of Jijel. His research interests include electromagnetic compatibility in electrical systems, electronic engineering and electrical power engineering, and molding control and integration of energy storage in ac and dc shipboard microgrids.

Chun-Lien Su (Senior Member, IEEE) received the Diploma degree in electrical engineering from the National Kaohsiung Institute of Technology, Kaohsiung City, Taiwan, in 1992, and the M.S. and Ph.D. degrees in electrical engineering from the National Sun Yat-sen University, Kaohsiung, Taiwan, in 1997 and 2001, respectively.

In 2002 and 2006, he was an Assistant Professor and an Associate Professor with the Department of Marine Engineering, National Kaohsiung Marine University, Kaohsiung, respectively, where he was as a Full Professor from 2012 to 2017 and the Director of the Energy and Control Research Center. From August 2017 to January 2018, he was a Visiting Professor with the Department of Energy Technology, Aalborg University, Aalborg, Denmark. He was the Director of Maritime Training Center, National Kaohsiung University of Science and Technology (NKUST), Kaohsiung, from February 2018 to July 2020. Since August 2020, he has been a Professor with the Department of Electrical Engineering, NKUST, where he is also the Director of Center for Electrical Power and Energy. His research interests include power system analysis and computing, power quality, maritime microgrids, and offshore energy, recently specially focused on electrical infrastructure for offshore wind farms and maritime microgrids for electrical ships, vessels, ferries, and seaports.

Dr. Su received the Best Paper Prize of the Industrial & Commercial Power Systems Conference at the IEEE Industry Applications Society (IAS) for the period 2012–2013 and the Best Paper Award of the IEEE International Conference on Smart Grid and Clean Energy Technologies in 2018. He was a Guest Editor of the IEEE TRANSACTIONS ON INDUSTRIAL INFORMATICS Special Issues: Next Generation Intelligent Maritime Grids in 2017 and the *IET Renewable Power Generation* Special Issues: Power Quality and Protection in Renewable Energy Systems and Microgrids in 2019.

Josep M. Guerrero (Fellow, IEEE) received the B.S. degree in telecommunications engineering, the M.S. degree in electronics engineering, and the Ph.D. degree in power electronics from the Technical University of Catalonia, Barcelona, Spain, in 1997, 2000, and 2003, respectively.

Since 2011, he has been a Full Professor with the Department of Energy Technology, Aalborg University, Aalborg, Denmark, where he is responsible for the Microgrid Research Program. Since 2014, he has been a Chair Professor with Shandong University, Jinan, China. Since 2015, he has been a Distinguished Guest Professor with Hunan University, Changsha, China. Since 2016, he has been a Visiting Professor Fellow with Aston University, Birmingham, U.K., and a Guest Professor with the Nanjing University of Posts and Telecommunications, Nanjing, China. In 2019, he became a Villum Investigator. He has published more than 500 journal articles in the fields of microgrids and renewable energy systems, which are cited more than 30 000 times. His research interests include different microgrid aspects, including power electronics, distributed energy-storage systems, hierarchical and cooperative control, energy management systems, smart metering, and the Internet of Things for ac/dc microgrid clusters and islanded minigrids, recently specially focused on maritime microgrids for electrical ships, vessels, ferries, and seaports.

Dr. Guerrero was elevated as an IEEE Fellow for his contributions on "distributed power systems and microgrids" in 2015. He received the Best Paper Award of the IEEE TRANSACTIONS ON ENERGY CONVERSION for the period 2014–2015 and the Best Paper Prize of the IEEE Power and Energy Society (PES) in 2015. He also received the Best Paper Award of the *Journal of Power Electronics* in 2016. During five consecutive years, from 2014 to 2018, he was awarded by Clarivate Analytics (former Thomson Reuters) as a Highly Cited Researcher. He is also an Associate Editor for a number of the IEEE TRANSACTIONS.

Juan C. Vasquez (Senior Member, IEEE) received the B.S. degree in electronics engineering from the Autonomous University of Manizales, Manizales, Colombia, in 2004, and the Ph.D. degree in automatic control, robotics, and computer vision from the Polytechnic University of Catalonia (BarcelonaTech-UPC), Barcelona, Spain, in 2009.

He was a Visiting Scholar with the Center of Power Electronics Systems (CPES), Virginia Polytechnic Institute and State University (Virginia Tech), Blacksburg, VA, USA, and a Visiting with Ritsumeikan University, Kyoto, Japan. In 2011, he was an Assistant Professor and in 2014, an Associate Professor with the Department of Energy Technology, Aalborg University, Aalborg, Denmark. In 2019, he became a Professor of energy Internet and microgrids with the Villum Center for Research on Microgrids, Aalborg University, where he is currently the Co-Director. He has published more than 450 journal articles in the field of microgrids, which, in total, are cited more than 19 000 times. His current research interests include operation, advanced hierarchical and cooperative control, optimization and energy management applied to distributed generation in ac/dc microgrids, maritime microgrids, advanced metering infrastructures, and the integration of the Internet of Things and the energy Internet into the smartgrid.

Prof. Vasquez is also a member of the IEC System Evaluation Group SEG4 on LVDC Distribution and Safety for Use in Developed and Developing Economies, the Renewable Energy Systems Technical Committee TC-RES in the IEEE Industrial Electronics Society (IES), the IEEE Power Electronics Society (PELS) Society, the IEEE Industry Applications Society (IAS) Society, and the IEEE Power and Energy Society (PES) Society. He was awarded as the Highly Cited Researcher by Thomson Reuters from 2017 to 2019. He was a recipient of the Young Investigator Award 2019. He is also an Associate Editor of the *IET Power Electronics* and a Guest Editor of the IEEE TRANSACTIONS ON INDUSTRIAL INFORMATICS Special Issue on Energy Internet.

Saeed Golestan (Senior Member, IEEE) received the B.Sc. degree in electrical engineering from Shahid Chamran University of Ahvaz, Ahvaz, Iran, in 2006, the M.Sc. degree in electrical engineering from the Amirkabir University of Technology, Tehran, Iran, in 2009, and the Ph.D. degree in electrical engineering from Aalborg University, Aalborg, Denmark, in 2018.

He is currently an Assistant Professor with the Department of Energy Technology, Aalborg University. His research interests include synchronization and signal processing techniques in power applications, and modeling and control of power converters.